

UKAEA-CCFE-CP(19)50

Maria Lorena Richiusa, Wayne Arter, Dominic Calleja, Medhi Firdaouss, Jonathan Gerardin, Michael Kovari, Francesco Maviglia, Zsolt Vizvary

# **DEMO First Wall misalignment study by 3D field line tracing**

This document is intended for publication in the open literature. It is made available on the understanding that it may not be further circulated and extracts or references may not be published prior to publication of the original when applicable, or without the consent of the UKAEA Publications Officer, Culham Science Centre, Building K1/O/83, Abingdon, Oxfordshire, OX14 3DB, UK.

Enquiries about copyright and reproduction should in the first instance be addressed to the UKAEA Publications Officer, Culham Science Centre, Building K1/O/83 Abingdon, Oxfordshire, OX14 3DB, UK. The United Kingdom Atomic Energy Authority is the copyright holder.

The contents of this document and all other UKAEA Preprints, Reports and Conference Papers are available to view online free at [scientific-publications.ukaea.uk/](https://scientific-publications.ukaea.uk/)

# **DEMO First Wall misalignment study by 3D field line tracing**

Maria Lorena Richiusa, Wayne Arter, Dominic Calleja, Medhi  
Firdaouss, Jonathan Gerardin, Michael Kovari, Francesco  
Maviglia, Zsolt Vizvary



# DEMO Single Module Segment Concept First Wall and limiter misalignment study by 3D field line tracing

Maria Lorena Richiusa<sup>a</sup>, Wayne Arter<sup>a</sup>, Dominic Calleja<sup>b</sup>, Mehdi Firdaouss<sup>c</sup>, Jonathan Gerardin<sup>c</sup>, Michael Kovari<sup>a</sup>, Francesco Maviglia<sup>d</sup>, Zsolt Vizvary<sup>a</sup>

<sup>a</sup>UKAEA-CCFE, Culham Science Centre, Abingdon, Oxon, OX14 3DB, UK

<sup>b</sup>University of Liverpool, Liverpool, UK

<sup>c</sup>IRFM CEA Cadarache, 13108, Saint Paul lez Durance, France

<sup>d</sup>EUROfusion – Programme Management Unit, Boltzmannstrasse 2, 85748 Garching, Germany

Within the framework of EUROfusion DEMO First Wall and limiter design activities, the protection of the First Wall against power deposition peaks is being considered. During steady-state operation, the radiative power from the plasma could be considered uniformly spread on plasma-facing components. However, the presence of openings (i.e. gaps between segments and ports) and the introduction of limiters breaks the continuity of the wall and opens the possibility of localized high heat flux values on toroidally facing gaps due to charged particles striking the wall. These fluxes can be amplified by misalignments between components upon manufacturing, assembly or under operational conditions.

In this paper, the 3D field line tracing code SMARDDA is used for studying the impact of misalignment on the heat load distribution for a periodically segmented DEMO First Wall, specifically the Single Module Segment Concept. The work covers normal operation conditions (ramp-up and steady-state), considering both the cases of bare First Wall (without limiters, as reference) and First Wall protected by limiters. The main aim of the work is understanding how the power deposition on the First Wall (due to charged particles) is affected by the presence of a radial or vertical misalignment between segments and starting a workflow to be applied later to all the possible plasma scenarios and FW layout. Heat flux penalty factor maps have been created to identify the worst cases among the ones analyzed. The related heat flux maps are relevant for thermal assessments of a simplified DEMO model to be performed later on, particularly in terms of maximum temperature values for the current DEMO design.

Keywords: Misalignment Study, SMARDDA, 3D Field Line Tracing, Single Module Segment Concept.

## 1. Introduction

The intrinsic EUROFER97 engineering limit on maximum temperature (550°C) poses a threshold on the DEMO First Wall (FW) admissible heat flux peak (~1 MW/m<sup>2</sup>) during the plasma pulse flat-top phase [1].

The DEMO Plasma-Facing Components (PFCs) are exposed to charged particle heat loads, fast particle loads, radiative loads, and heat loads from disruption events. The power deposition due to charged particles flowing along magnetic field lines ( $Q_{||}$ ) leads to a non-uniform heat flux map on the PFCs, above all in a segmented FW that exposes the toroidal-faced edges to the magnetic field lines [2]. Since the heat flux magnitude strongly depends on two main factors, i.e. the heat load along field lines and the angle between the magnetic field  $B$  and the PFC surface normal, a dedicated shaping and chamfering of the FW front face can help reduce the power density peaks to allowable engineering limits on the PFC surface.

Within the framework of EUROfusion DEMO First Wall and limiter design activities, experience of what has been done for protecting ITER FW against localized power deposition peaks [3] has led to similar and more simplified approaches [4] for shaping the DEMO Single Module Segment (SMS) FW [5] and shadowing its exposed edges accordingly in such a way to prevent the

FW from localized hot spots that could compromise its structural integrity for entire working life.

Furthermore, the strategy adopted for handling the huge amount of energy released by the plasma during off-normal plasma events (such as disruptions, VDEs) foresees a set of localized limiters [6]. Four limiters prevent the plasma touching the FW by protruding from it, reducing at the same time the heat flux magnitude on the neighboring segments.

Apart from the toroidal discontinuity of the FW, localized power density peaks could also be caused by misalignment between components upon manufacturing, assembly, disruption-induced loads or under operational conditions (i.e. different thermal expansions could lead to different displacements between adjacent segments leaving edges exposed to the magnetic field lines). High surface temperatures localized at the edges of tiles increase the risk of material evaporation and sputtering, with the potential of plasma contamination, while inducing high thermo-mechanical stresses on the components which could compromise their integrity. For these reasons, a study focused on the investigation of the effects of the above-mentioned misalignments between segments has started in order to understand tolerances and power density peaks due to misaligned segments under charged particle heat load, using the in-house field-line

tracing SMARDDA-PFC code [7] under different plasma scenarios foreseen for EU DEMO. The study is carried out taking into consideration both the bare FW and the concept of FW equipped with limiters, and in both cases the effect that the radial or vertical misalignment of each segment has on the neighboring segment's power deposition peak is investigated.

## 2. SMARDDA software

SMARDDA is a library of Object-Oriented Fortran-95 modules for ray, particle and field line tracing. This software library is used to perform design-relevant calculations for PFCs studying the interaction between charged particles magnetic field lines and complex engineered surfaces, in both limiter and divertor cases. SMARDDA-PFC is the field-line code adopted by ITER as part of the SMITER code package (SMARDDA for ITER) [8]. SMARDDA approach is based on following the field lines arising from the geometry towards the nominal source of power located at the tokamak midplane. In the case that their trajectories first strike the neighbouring wall this is regarded as shielding the launch point geometry [7]. The plasma scenario magnetic configuration is provided by means of EQDSK files. The model used for computing the power deposition is based on the Eich's two parameter exponential formula [9], the power in the Scrape-Off layer (SOL) and the power decay length ( $\lambda_q$ ) at the midplane.

## 3. Misalignment study

### 3.1 90° sector DEMO FW geometry

As far as the input geometries are concerned, they are built by using a combination of ANSYS modules (Workbench and APDL) for creating the Finite Element models of the 90° sector of DEMO FW (i.e. four 22.5° sectors of the DEMO FW Design 6b [10] joined together), taken as a reference for every run and considering a cyclic periodicity of four. Fig. 1 and Fig. 2 give an overview of the reference layout of the geometry without and with limiters, respectively.

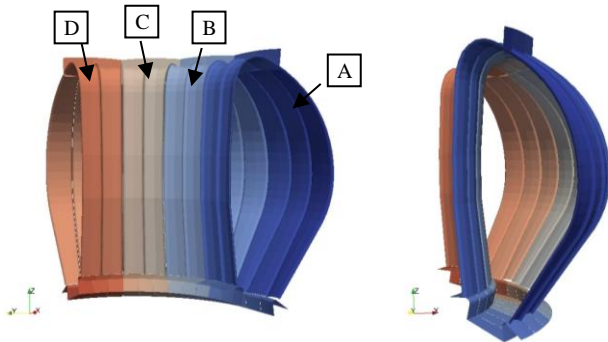


Fig. 1. 90° sector of DEMO bare FW.

Every 22.5° sector belonging to the 90° sector is identified with the labels A-D (Fig. 1) along the clockwise direction, while the following acronyms UL, OML, OLL, IML and UL\_II (Fig. 2) are used for labelling the limiters located in sectors A and C. An in-house APDL script set up ad hoc has been used for storing all the information related to the Finite Element models of each segment into vtk [11] file format (SMARDDA input files).

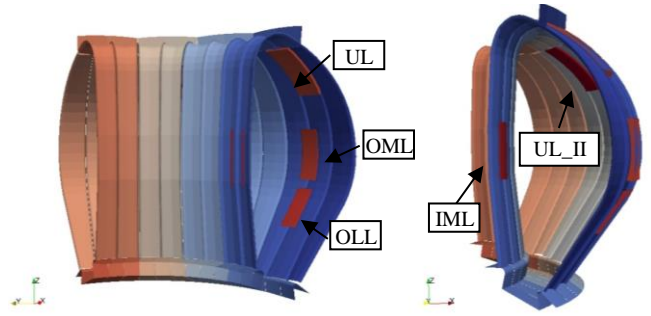


Fig. 2. 90° sector of DEMO FW equipped with limiters.

The displacements of the single segments for generating the misalignment cases have been done by means of a python script capable to manipulate the node coordinates contained in the vtk files previously generated and then letting SMARDDA deal with the assembly of the different segments by means of its implemented vtkfm module [12].

### 3.2 Plasma Scenarios and configurations analyzed

As far as the plasma scenarios are concerned, the plasma magnetic equilibria related to the Ramp-up (RU) [13] and Start-Of-Flat-top (SOF) [14] phases are taken into account for this study. The contour plots of these scenarios are shown in Fig. 3.

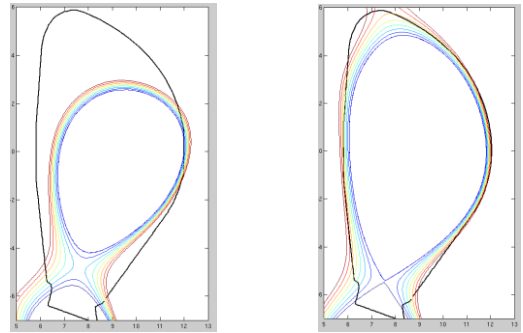


Fig. 3. 2D plasma magnetic equilibria during the RU (left-hand side) and the SOF (right-hand side) scenarios.

The RU is a preliminary phase before the formation of the X-point, when the SOF begins. During the RU, the limited plasma moves towards the outboard wall and the power into the SOL is foreseen to be  $P_{RU}=3.5$  MW against the  $P_{SOF}=69$  MW for the diverted configuration.

In terms of power balance, Table 1 shows the comparison between the total power input and the SMARDDA integrated power output obtained for the two reference configurations of the FW under the analyzed scenarios. The introduction of protruding components such as the limiters inside the bare FW creates a missing power issue as explained in [15]. For recovering the missing power, the heat flux peaks in Fig. 5 and Fig. 7 have been rescaled by the inverse of the ratio in Table 1.

Table 1. Integrated power calculated by using SMARDDA-PFC for the plasma scenarios analyzed.

Scenario	$Q_{REF}$ [MW]	$Q_{BARE\_FW}$ [MW]	Ratio	$Q_{FW\_LIM}$ [MW]	Ratio
RU	3.5	3.00	0.86	1.55	0.44
SOF	69	67	0.97	67	0.97

Fig. 4 shows the power deposition distribution, calculated by SMARDDA, on both the configurations of bare FW and FW with limiters during the RU. The maximum values of the heat flux on every component of the FW, in both the two configurations analysed, are collected in Fig. 5. It can be observed how the introduction of the OML plays an important role in mitigating the power deposition peak on the FW. Fig. 6 shows the heat flux distribution on the bare FW and on the FW equipped with limiters during the SOF. The related heat flux peaks are reported in Fig. 7. A decrease in the FW heat flux peaks can be also observed for the SOF where the IML and the UL contribute to lower the heat load on the inboard wall and on the upper part of the outboard segments.

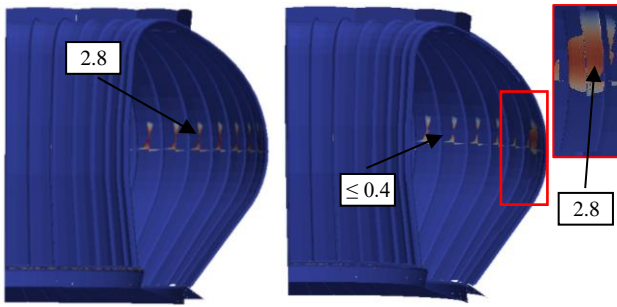


Fig. 4. Power deposition ( $\text{MW}/\text{m}^2$ ) during the RU scenario for the bare FW (left-hand side) and FW equipped with limiters (right-hand side).

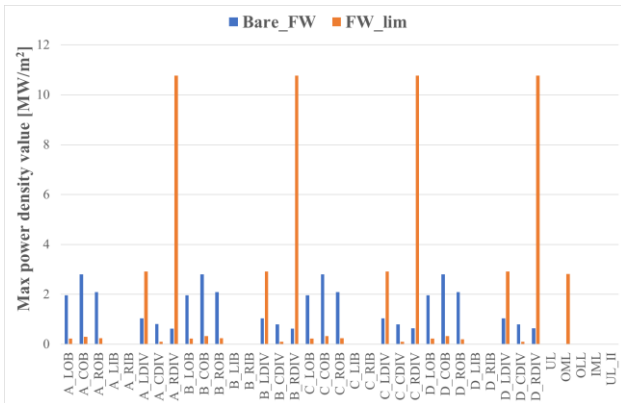


Fig. 5. Heat load peaks on both the bare FW and FW equipped with limiters during the RU phase.

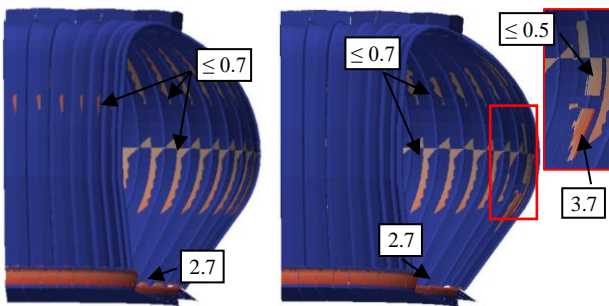


Fig. 6. Power deposition ( $\text{MW}/\text{m}^2$ ) during the SOF for the bare FW (left-hand side) and FW equipped with limiters (right-hand side).



Fig. 7. Heat load peaks on both the bare FW and FW equipped with limiters during the SOF phase.

For the misalignment study, under the RU and SOF heat loads described and for both the two FW configurations, the effect of the radial and vertical rigid body movement of all the segments belonging to sector A on the heat flux peak distribution have been investigated. Four different radial displacement values have been considered for every segment of the sector A with respect to its nominal position: +10/+20 mm outward, -10/-20 mm inward. This is valid for the outboard segment, whereas the translation must be interpreted in the opposite direction when referred to the inboard segments. The same values have been used for the vertical misalignment, that is +10/+20 mm upward and -10/-20 mm downward.

### 3.3 Results

Here is a summary of the results obtained, in terms of maximum heat flux values of the power deposition on both the displaced and the neighboring segments directly affected by the displacement of the first ones.

#### 3.1 Radial misalignment

Fig. 8-9 and Fig. 10-11 show the results related to the radial misalignment cases for the RU and SOF scenarios, respectively.

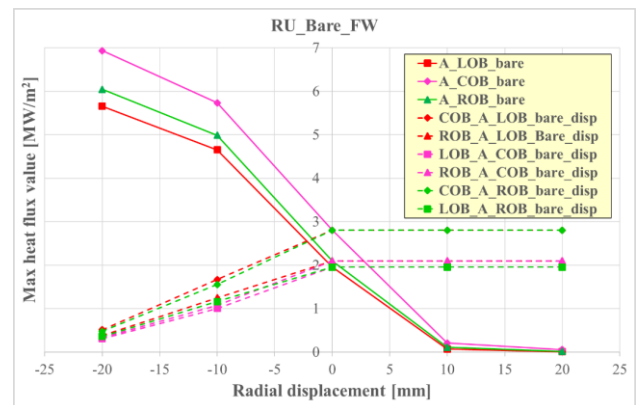


Fig. 8. Maximum heat flux values on the misaligned bare FW during RU scenario. Every misaligned segment is associated with a pointer shape and color. The neighboring segments (dotted lines) directly affected by the misaligned segment are pointed out by using their own shape pointer but filled with the color belonging to the misaligned segment.

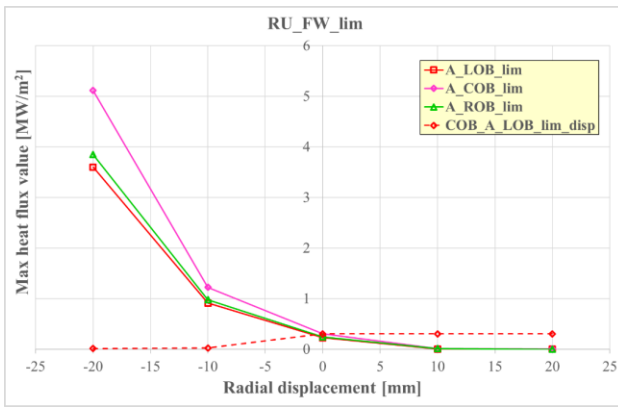


Fig. 9. Maximum heat flux values on the misaligned FW equipped with limiters during the RU plasma scenario. The way the data are displayed is explained in Fig. 8 caption.

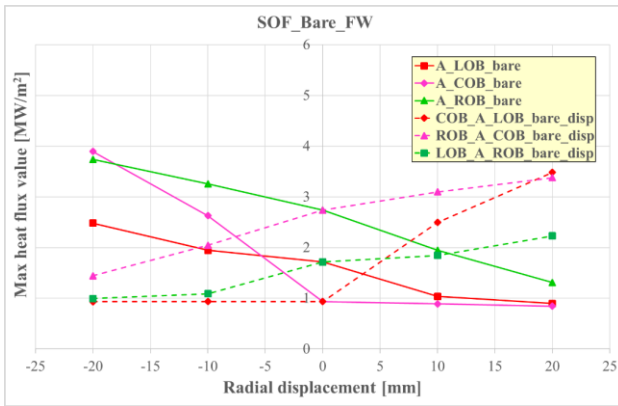


Fig. 10. Maximum heat flux values on the misaligned bare FW during the SOF plasma scenario. The way the data are displayed is explained in Fig. 8 caption.

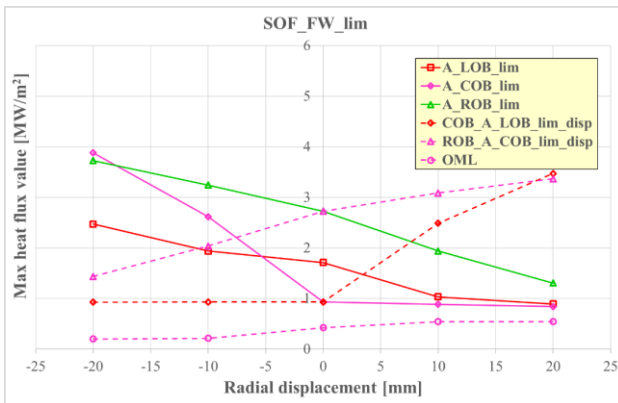


Fig. 11. Maximum heat flux values on the misaligned FW equipped with limiters during the SOF plasma scenario. The way the data are displayed is explained in Fig. 8 caption.

For the two plasma scenarios analyzed, since the radial and vertical misalignments of the inboard segments have not shown any significant change in the power deposition peaks, the results related to those cases have not been reported. The same rationale has been adopted for all the segments whose heat flux peak value is not affected by the presence of any misaligned segment.

Overall, the heat flux peak value decreases far below the engineering limit on the FW outboard segments as they are pushed outwards. During the RU the heat load peak is located in the equatorial midplane and its

magnitude increases with the protrusion of the segment towards the plasma. This effect is more evident in the bare FW where the power deposition peak reaches values close to  $5 \text{ MW/m}^2$  if a segment is moved inward by 10 mm. In case of FW with limiters, since the OML contributes to lower the magnitude of the heat load reaching the segments, the presence of a misaligned segment by 10 mm can increase the power deposition peak up to  $1 \text{ MW/m}^2$ .

During the SOF, with the FW design taken into account, the power deposition peaks are always located at the bottom of the outboard segments and exceed the engineering limit. For this reason, the obtained power deposition distribution is not so different for both the cases of bare FW and FW with limiters in the presence of misaligned segments, and the effect of a displaced segment is an increase in the peak magnitude. This suggests the need of a strategy for mitigating the power deposition in the bottom part of the outboard segments due to charged particles. Among all of the possible solutions, the one that is under investigation foresees pushing outwards by more than 20 mm and/or tilting the bottom surfaces of the outboard segments in such a way of having leading edges' shadowing the closest neighbors along the toroidal direction [16]. This strategy has been sketched with the aim of reducing the heat load on PFCs at least below the engineering limit.

The penalty factors  $f$  [17]-[18] are calculated for every segment by taking into account only the charged particle heat flux peak values reached in each segment for every case and comparing it with the peak value related to the aligned FW. For the RU case, both the bare FW and the FW with limiters show penalty factors close to unity for every segment except for the displaced segments of the outboard wall. In the bare FW, those displaced segments have  $f$  values close to 2.4/2.9 for an inward misalignment of 10/20 mm, respectively. When the limiters are introduced, the same  $f$  reaches values of 4/15 for 10/20 mm misalignment since the reference peak is lower than the related bare FW heat flux peak. The inboard segments always experience unity  $f$  since they are not affected by any radial misalignment during the RU. For sake of brevity, only the  $f$  related to the SOF are displayed. Fig. 12 shows the  $f$  calculated for the FW with limiters only for the worst misaligned cases (same trend for the bare FW).

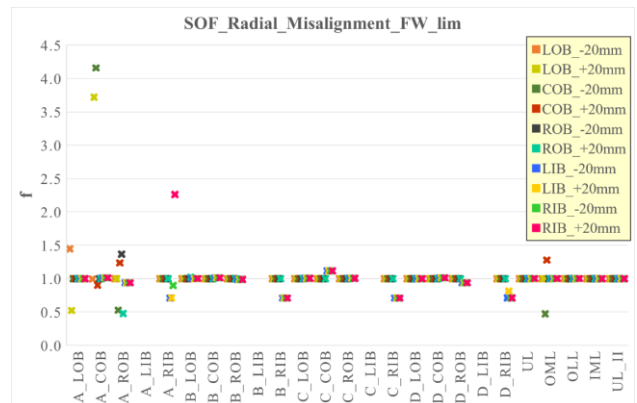


Fig. 12. Segment penalty factors for the SOF.



### 3.2 Vertical misalignment

The results related to the vertical misalignment cases are in Fig. 13-14 (RU) and Fig. 15-16 (SOF). It can be said that a vertical misalignment of one segment during RU doesn't significantly affect the heat load peaks on its neighboring segments in the case of bare FW. The peaks are always located at the outboard equatorial midplane and the peak value increases in magnitude on the misplaced outboard segments as these segments are moved downward from their nominal position. In the case of a FW equipped with limiters, the FW heat flux peak is always below the engineering limits, by ensuring a large margin of tolerance even when the segment is displaced with respect to its reference position for whatever reason.

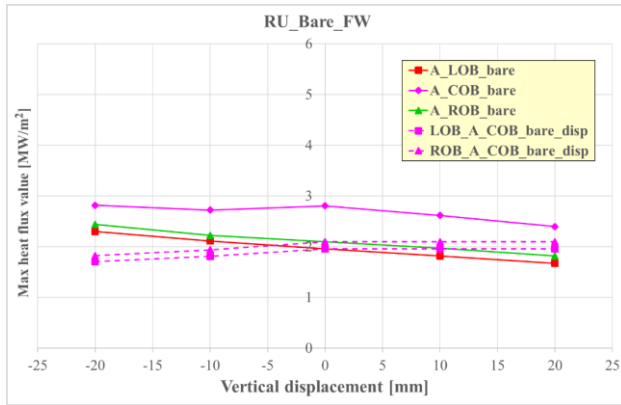


Fig. 13. Maximum heat flux values on the misaligned bare FW during the RU plasma scenario. The way the data are displayed is explained in Fig. 8 caption.

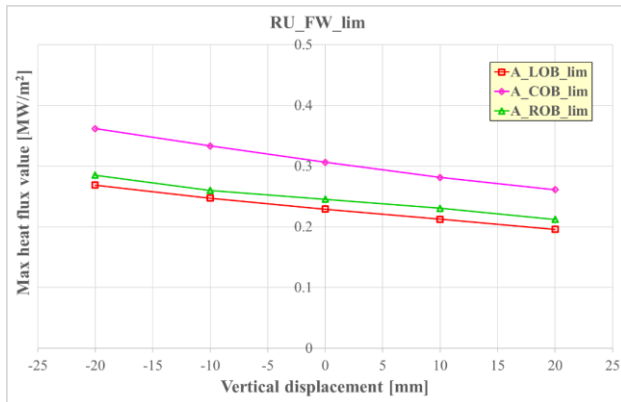


Fig. 14. Maximum heat flux values on the misaligned FW equipped with limiters during the RU plasma scenario. The way the data are displayed is explained in Fig. 8 caption.

As far as the SOF is concerned, what has been said for the radial misalignment cases is still valid for the vertical misaligned cases, i.e. the peak heat load on the outboard segments is always located at their bottom surfaces and this makes the power distribution map not so different for the two reference FW configurations analyzed. In this case, though, the vertical displacement of one segment has the effect of increasing its maximum heat flux value which moves closer to the left-hand side edge of the bottom part of the segment as the misalignment increases. Looking at the data in Fig. 15 and Fig. 16, an upward displacement of the LOB increases the heat flux peak on the COB while a downward displacement of the COB

increases the peak heat flux of the ROB. As already said in §3.1, the vertical misalignment of the two inboard segments doesn't affect the heat flux map. However, when the right inboard segment moves 20 mm downward, its bottom surface close to its right-hand corner experiences a peak of 1.44 MW/m<sup>2</sup>. Nonetheless, the right inboard segment's vertical displacements don't affect the power deposition on the left inboard segment.

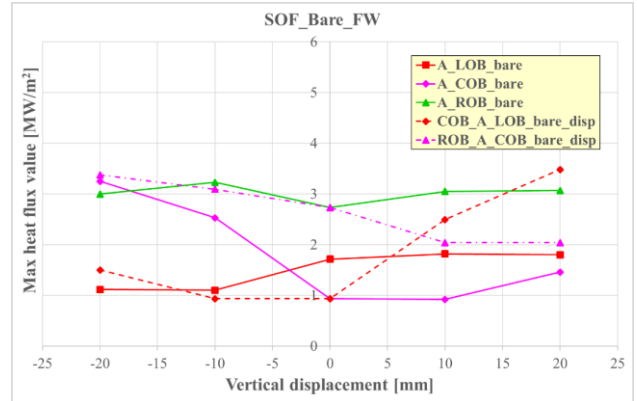


Fig. 15. Maximum heat flux values on the misaligned bare FW during the SOF plasma scenario. The way the data are displayed is explained in Fig. 8 caption.

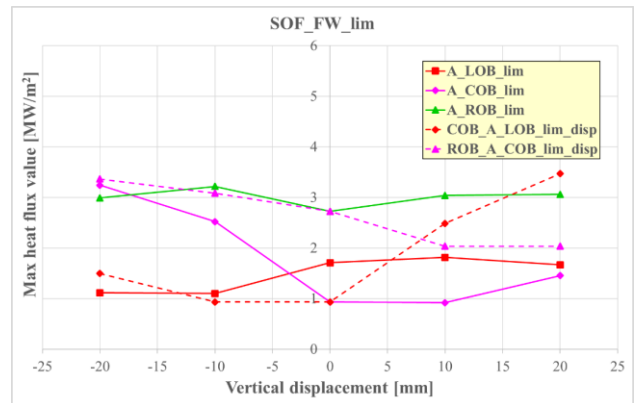


Fig. 16. Maximum heat flux values on the misaligned FW equipped with limiters during the SOF plasma scenario. The way the data are displayed is explained in Fig. 8 caption.

For the RU scenario, the  $f$  values in this case are always close to unity, going up to 1.1/1.2 for the outboard misaligned segments when they move 10/20 mm inwards, respectively. The  $f$  values related to the FW equipped with limiters during the SOF are reported in Fig. 17 only for the worst misaligned cases. Those values give an estimate about the bare FW penalty factors as well, since the difference between the heat flux map on the two reference geometries is negligible for the SOF.

This study paves the way to the investigation of the effects of different misalignment cases (i.e. rotation of a segment with respect to its toroidal and/or poloidal axis, misalignment due to thermal deformation of the segment and so on) as well as considering further plasma transient scenarios which could lead to either modify the FW shape or to find optimal protrusions for the limiters and provide information for the designers for the required tolerance levels that needs to be ensured during manufacturing and assembly. The work presented here only considers the

change in the peak heat flux magnitude but can be used to assess the thermal and structural behavior of the given components.

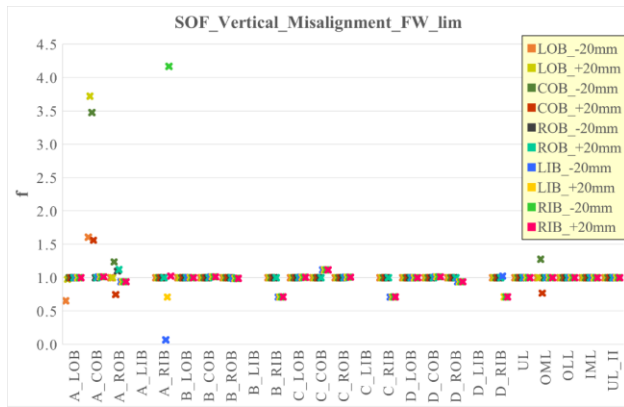


Fig. 17. Segment penalty factors for the SOF.

#### 4. Conclusions

The comparison between the power distribution due to charged particles on the bare FW and the FW equipped with the current layout of the limiters shows that the presence of limiters helps decrease the heat flux magnitude on the FW. The OML plays a crucial role in decreasing the heat flux on the segments during the RU phase (Fig. 3) while all the limiters contribute to the FW segment shadowing during the SOF (Fig. 4). The limiter FW configuration allows for  $\pm 10$  mm segment displacement tolerance both in the radial and vertical directions during the RU phase whereas the same cannot be stated for the SOF phase as the power deposition peak is located at the bottom surface close to the divertor baffle. However, since the SOF is foreseen to be the normal operation and PFCs have to withstand the heat load during the SOF for longer, misalignment tolerances should be mainly allowed during SOF, meaning that the current FW design needs to be modified in order to limit the charged particle heat flux peak below the engineering limit. The strategy currently followed foresees the tilting of the outboard segment bottom surfaces for shadowing their toroidal neighbourhoods in order to reduce the heat load peak on FW acting on both increasing its distance from the plasma and shaping its front face.

#### Acknowledgments

This work has been carried out within the framework of the EUROfusion Consortium and has received funding from the Euratom research and training programme 2014-2018 and 2019-2020 under grant agreement No 633053. The views and opinions expressed herein do not necessarily reflect those of the European Commission.

#### References

[1] T. Barrett et al., Technologies for plasma-facing wall protection in EU DEMO, 27th IAEA Fusion Energy Conference – IAEA CN-258, Gandhinagar (Ahmedabad) Gujarat, India, October 22-27, 2018.  
 [2] DEMO PFC Heat Load Specification, <https://idm.eurofusion.org/?uid=2L6867>.  
 [3] P. Stangeby, The strong effects of gaps on the required

shaping of the ITER first wall, 2011 Nucl. Fusion 51 033008.  
 [4] M. Kovari, First Wall design principles, Report IDM reference No. 2MHN6W.  
 [5] M. L. Richiusa, First Wall 3-D surface design in conjunction with PMI Physics group, Report IDM reference No. 2MZMVS.  
 [6] C. Bachmann et al., Critical design issues in DEMO and solution strategies, Fusion Engineering and Design, <https://doi.org/10.1016/j.fusengdes.2018.12.013>.  
 [7] W. Arter et al., Power Deposition on Tokamak Plasma-Facing Components. IEEE Transactions on Plasma Science, Vol. 42, Issue 7, July 2014, pp. 1932-1942. [arXiv:1403.7142](https://arxiv.org/abs/1403.7142).  
 [8] L. Kos et al., SMITER: A field-line tracing environment for ITER. Fusion Engineering and Design, <https://doi.org/10.1016/j.fusengdes.2019.03.037>, in press.  
 [9] T. Eich et al., Inter-ELM Power Decay Length for JET and ASDEX Upgrade: Measurement and Comparison with Heuristic Drift-Based Model, Physical Review Letters, vol. 107, no. 21, p. 215001, 2011.  
 [10] DEMO FW Design 6a and b, IDM Reference No. 2LLHSR.  
 [11] Kitware, The VTK User's guide. Kitware Inc., Columbia, 2006, ch. File formats for VTK version 4.2, <http://www.vtk.org/VTK/img/file-formats.pdf>.  
 [12] SMARDDA/PFC User Manual.  
 [13] EQDSK\_RU\_RD\_RAPTOR\_Baseline2017\_Ip17d75\_2N9JRB\_v1\_0, IDM reference No. 2N9JRB.  
 [14] SN\_2017\_UVDE\_1\_c\_xpoint\_clockwise\_2NAC79\_v1\_0, IDM reference No. 2NAC79.  
 [15] J. Gerardin et al., Simplified heat load modeling for design of DEMO discrete limiters, Journal of Nuclear Materials, <https://doi.org/10.1016/j.nme.2019.01.002>.  
 [16] Z. Vizvary et al., European DEMO first wall shaping and limiters design and analysis status, *This conference*.  
 [17] R. Mitteau et al., The combined effects of magnetic asymmetry, assembly and manufacturing tolerances on the plasma heat load to the ITER first wall. Journal of Nuclear Materials, <http://dx.doi.org/10.1016/j.jnucmat.2014.12.102>.  
 [18] Z. Vizvary et al., DEMO First Wall misalignment study, Fusion Engineering and Design, <https://doi.org/10.1016/j.fusengdes.2019.04.046>.